Available online at www.sciencedirect.com
ScienceDirect
Advanced Drug Delivery Reviews 58 (2006) 788–808
Advanced DRUG DELIVERY Reviews
www.elsevier.com/locate/addr

Principles of two-photon excitation fluorescence microscopy and other nonlinear imaging approaches ☆

Martin Oheim [a,*], Darren J. Michael [b], Matthias Geisbauer [b], Dorte Madsen [b,1], Robert H. Chow [b]

[a] *Molecular and cellular Biophysics of the Synapse, INSERM U603, F-75006 Paris, France; Laboratory of Neurophysiology and New Microscopies, 45 rue des Saints Pères, F-75006 Paris, France*
[b] *Zilkha Neurogenetics Institute and Dept of Physiology and Biophysics, University of Southern California Keck Medical School, 1501 San Pablo Street, Los Angeles, CA 90089-2821, U.S.A.*

Received 22 May 2006; accepted 13 July 2006
Available online 9 August 2006

Abstract

The aim of this article is to review the basic principles of two-photon excitation fluorescence (2PEF) microscopy and to compare the advantages and disadvantages of 2PEF imaging to other microscopy methodologies. 2PEF imaging is a *nonlinear* approach that generates images of optical sections and that is particularly well suited for deep-tissue and *in vivo* imaging of live animals. The nonlinear excitation used for 2PEF offers the advantage, too, of being able to generate contrast from second or third harmonic generation as well as coherent anti-Stokes Raman scattering. We also review the recent use of nonlinear excitation to provide image resolution beyond the diffraction limit and discuss the progress in non-scanning (planar) 2PEF microscopy, an approach that holds great potential for large-scale quantitative imaging and plate reading, e.g., in screening applications.

Keywords: Two-photon excitation fluorescence (2PEF) microscopy; Coherent anti-Stokes Raman scattering; Planar 2PEF microscopy

Contents

1. Introduction 789
1.1. Nonlinear fluorescence excitation 789

☆ This review is part of the *Advanced Drug Delivery Reviews* theme issue on "Multi-Photon Imaging: Diseases and Therapies", Vol. 58/7, 2006.

* Corresponding author. Tel.: +33 1 42 86 42 21; fax: +33 1 42 86 41 51.
E-mail address: martin.oheim@univ-paris5.fr (M. Oheim).
[1] D.M. is now with the Department of Chemistry, University of California, Davis, One Shields Avenue, Davis, CA 95616, USA.

0169-409X/$ - see front matter © 2006 Elsevier B.V. All rights reserved.
doi:10.1016/j.addr.2006.07.005

2. Fluorescence as a contrast generator in biological images . . . 790
2.1. One-photon excitation fluorescence (1PEF) . . . 790
2.2. Epifluorescence excitation with wide-field detection . . . 791
2.3. Confocal detection . . . 792
2.4. Nonlinear microscopies . . . 792
3. Recent developments in nonlinear imaging . . . 795
3.1. Linking morphology and function in deep-tissue imaging . . . 796
3.2. Rapid, random-access scanning . . . 797
3.3. Fiber delivery of ultrashort nonlinear pulses . . . 798
3.4. Two-photon fiberscopes for imaging freely moving animals . . . 798
3.5. Chemical uncaging, ablation, histology and light-induced permeabilization . . . 799
3.6. New fluorophores . . . 800
3.7. Higher harmonic generation . . . 800
3.8. *C*oherent *a*nti-Stokes *R*aman *s*cattering (CARS) . . . 801
3.9. *S*timulated *e*mission *d*epletion (STED) microscopy . . . 802
3.10. Large-area (non-scanning) two-photon excitation . . . 804
4. Summary and conclusions . . . 805
Acknowledgements . . . 805
References . . . 805

1. Introduction

Complementing the molecular biology and proteomics revolutions, optical microscopy has evolved rapidly to become one of the most important biomedical research tools today. The chief reasons for this are the development and widespread availability of powerful new microscopy approaches and the introduction of genetically encoded fluorescent proteins, such as green fluorescent protein (GFP) and its spectral and functional variants. Together, these advances have enabled deep tissue imaging in living animals with unprecedented resolution and contrast and highly specific targeting of fluorescent biomarkers.

While confocal microscopy permits the acquisition of high-resolution three-dimensional (3-D) images of cultured cells and 'optically thin' specimens, its use for imaging deep in tissue is limited. This is because tissue is a hostile environment for light microscopy, due to the strong scattering of ultraviolet (UV) and visible light. In brain tissue, the effective *scattering length*, i.e., the average distance that a photon travels between two scattering events is on the order of 50–100 μm. As confocal microscopy relies on first concentrating excitation photons to a tight focus and then collecting and directing the emitted fluorescent photons through a detector pinhole, this technique is particularly vulnerable to scattering. Both on the excitation and emission (detection) side, only *ballistic* photons–i.e., photons that travel directly from *a* to *b* without being deflected–contribute to the useful signal. Worsening the problem, scattered excitation photons not only fail to contribute to the tight focus but they also excite diffuse fluorescence and cause photobleaching, too. These two effects combine to cause the rapid loss of both intensity and contrast in confocal images when focusing more than a few tens of μms into tissue. Thus, for all its virtues, the confocal light microscope has the major flaw that it makes inefficient use of both the excitation and emission light. For example, in a specimen of ~100-μm thickness, less than 1% of the excited fluorescence is actually used for confocal imaging.

1.1. Nonlinear fluorescence excitation

In the 1990s, when mode-locked infrared lasers turned from a finicky piece of equipment of physics laboratories into a commercial turn-key device [1], another optical sectioning method, based on nonlinear optics emerged: *multi-photon microscopy* is an approach to image fluorophores excited by the near-simultaneous absorption of two (or more) low-energy photons.

In common with other optical sectioning techniques like total internal reflection microscopy (TIRFM) or structured illumination, this approach uses the strategy of getting crisper images by restricting the fluorescence *excitation* volume, rather than restricting the fluorescence *collection* volume, as is done in confocal microscopy. Although one could in principle combine restricted fluorescence excitation and collection approaches, we will argue in Section 3 that restricting the fluorescence collection volume is detrimental to collecting the maximal signal in nonlinear microscopy, especially for deep-tissue imaging. We note that yet another important means of enhancing image quality is to restrict the "fluorophore volume" (i.e., specific targeting of the fluorophore to the structure of interest). Thus, combining the 'new microscopies' and the new tools of molecular biology offers cell biologists, neuroscientists and anatomists unprecedented power to image cellular structures and processes.

The aim of this article is to give an overview of nonlinear microscopy, sufficient to provide the reader with the background to understand the compendium of articles appearing in this volume on *in vivo* imaging. Although the field of multi-photon microscopy is in rapid expansion, there are several excellent reviews that give a fairly complete overview of different aspects of nonlinear microscopy [2–7].

We start by briefly discussing the basics of single-photon fluorescence excitation, then consider multi-photon excitation and the means of creating images by raster-scanning the multi-photon excitation volume across the specimen. We then discuss some alternative modes of imaging thin optical sections and compare their respective advantages and disadvantages. The review terminates with a perspective on the current frontiers in nonlinear imaging.

2. Fluorescence as a contrast generator in biological images

Fluorescence has been used extensively to generate and enhance contrast in biological samples that, due to their low refractive-index variations, present little contrast. A detailed discussion of the basis of fluorescence microscopy is beyond the scope of this article. We review just the essentials in as much as they are necessary for understanding the concepts of nonlinear fluorescence excitation. For further reading, many free tutorials on fluorescence are found online (see, e.g., [8], also the websites of major microscope manufacturers, e.g., www.microscopyu.com, www.olympusmicro.com, etc.). An exhaustive and very didactic treatment of general fluorescence is found in the classical book of Lakowicz [9]. A concise review of fluorescence techniques as applied to drug delivery research is found in an earlier volume of this journal [10].

2.1. One-photon excitation fluorescence (1PEF)

Fluorescence occurs when a photon is absorbed by a fluorophore, raising an electron to an excited energy state, from which it relaxes to the electronic ground state and emits a lower energy photon. For absorption to occur, the energy of the exciting photon has to approximately match the energy difference between the excited state and the ground state (Fig. 1A). At room temperature, absorption of a photon takes place from the vibrational ground state S_0 within $\sim 10^{-18}$ s. Photon absorption excites the molecule to the singlet state S_2 from which it undergoes a radiation-less loss of energy by internal conversion to reach S_1.

From S_1, there are several possible fates. By far most molecules will return to the electronic ground state without emitting a photon. Their electronic energy will be transferred to the surroundings and converted into heat when molecules collide. However, in some cases, after a delay of $\sim 10^{-8}$–10^{-9} s, the electron drops back to the ground state and a photon is emitted. This emitted fluorescent photon is of lower energy (i.e., longer wavelength) than the photon originally absorbed, a phenomenon known as the *Stokes shift*. The *fluorescence lifetime* refers to duration of time between absorption of an excitation photon and the emission of a fluorescent photon. The fluorescence lifetime is typically exponentially distributed and is highly sensitive to the fluorophore environment and, therefore, may be used to report changes in the local fluorophore environment.

From S_1, another possible fate is to emit a phosphorescent photon. In this case, the excited electron undergoes intersystem crossing (ISC) to attain the triplet state, before it exits to the ground state. The lifetime of the excited state in phosphorescence is significantly longer than that in fluorescence—on the order of $\sim 10^{-4}$ s to minutes or even hours. The drop to the ground state is accompanied by emission of a

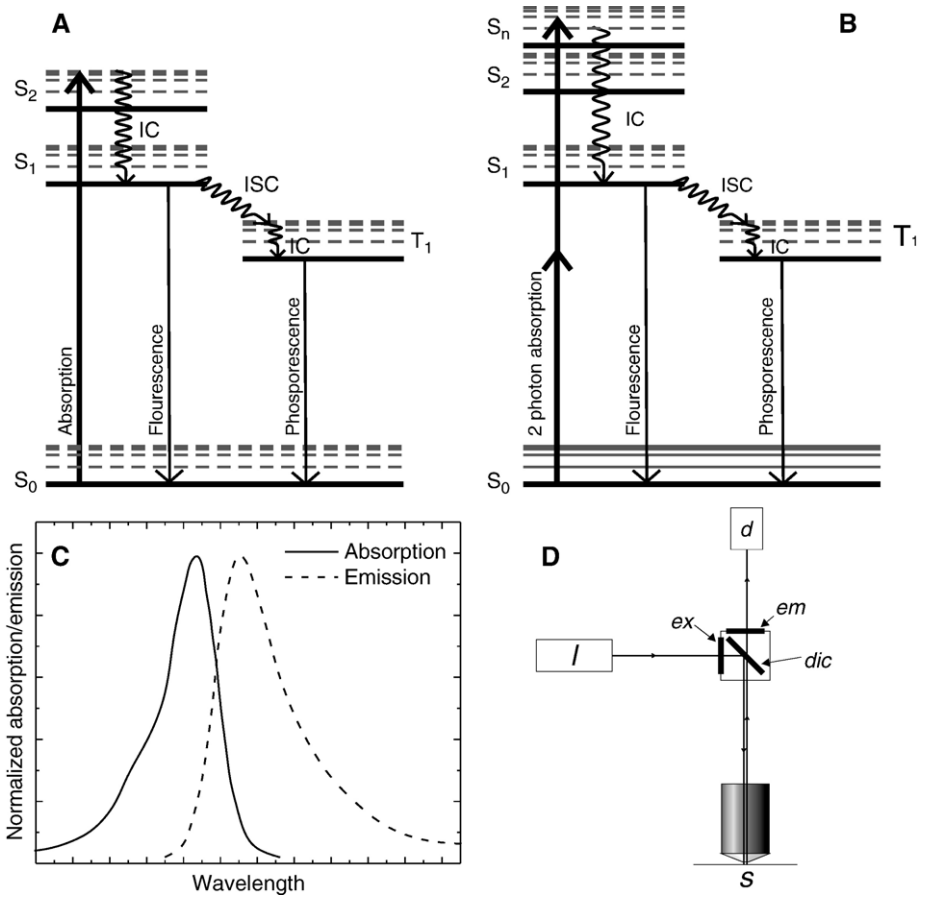

Fig. 1. (A) Jablonski diagram of single-photon excitation. The electronic energy levels and their vibrational substructure are shown with horizontal lines, and the physical processes that cause transitions between these levels are depicted by vertical arrows. The singlet ground, first and second electronic states are labeled S_0, S_1 and S_2, respectively, and the first triplet state is labeled T_1. For each of these electronic states, the molecule can exist in a multitude of vibronic states indicated by the dashed lines. (B) Jablonski diagram of multi-photon excitation (2PEF). (C) Schematic drawing of the absorption and fluorescence emission spectra of a fluorophore. Spectra are normalized to peak absorption and emission, respectively. (D) Block diagram of a typical epifluorescence microscope. *l*—light source, *ex*—excitation band-pass filter, *dic*—dichroic mirror, *s*—sample, *em*—emission (band-pass or long-pass) filter, *d*—detector.

photon, also of lower energy than the exciting photon.

For each of these processes, a *quantum yield* can be defined that quantifies the relative importance of a given decay pathway. For example, the fluorescence quantum yield specifies the fraction of excited states that relaxes via the emission of a fluorescence photon. The parameters that characterize a molecule's capacity for light absorption and fluorescence emission are the *molar extinction* ε (measured at peak absorption per mole and cm of optical path-length) and absorption spectrum and the *fluorescence quantum yield* ϕ (dimensionless) and emission spectrum, respectively (Fig. 1C). The brightness of a fluorophore is hence determined by the product $\varepsilon\phi$.

2.2. Epifluorescence excitation with wide-field detection

In comparison with bright-field (transmitted, reflected light) techniques, fluorescence microscopy derives its improved contrast from the specific labeling of subcellular structures of interest with a fluorescent marker and from the rejection of unwanted, short-wavelength

background by spectrally filtering the longer-wavelength, emitted light [10]. As such, fluorescence microscopy depends fundamentally on the Stokes shift. In the excitation pathway (Fig. 1D), broadband light emitted by a light source such as a Xenon or Mercury arc lamp is passed through a filter (excitation filter) that (ideally) transmits only wavelengths matched to the absorption spectrum of the fluorophore and directed (reflected at a 90° angle) onto the sample using a wavelength-dependent (dichroic) mirror. Alternatively, an expanded laser beam can provide monochromatic excitation. The fluorescence photons arising from the sample enter the emission pathway, which includes again the dichroic (this time transmitting the longer-wavelength fluorescence) and another filter (emission or blocking filter) that blocks the shorter excitation wavelength, so only the longer-wavelength fluorescence photons are collected at a detector. In wide-field imaging, photons are collected through a microscope objective and one or more lenses that ultimately focus the emitted light onto a detector, typically a CCD camera. However, not only photons arising from the focal plane are collected. Photons are collected also from out-of-focus planes, resulting in some blurring of the outlines of regions of interest in the image and limiting the effective optical sectioning power of wide-field microscopy.

2.3. Confocal detection

Confocal microscopy was developed to remove the out-of-focus light [11]. It is based on the recognition that when an illumination point source (i.e., light emerging from a pinhole) is focused to a diffraction-limited spot in the sample, this in-focus spot is represented again as a point in the focal plane of an imaging (tube) lens (Fig. 2A). The illumination and detection pinholes and the in-focus spot in the sample are said to be "con-focal". A detection pinhole positioned precisely at the focus of the image lens will selectively pass the light collected from the confocal point in the sample, but it will exclude most of the light arising from non-confocal points, both from within the specimen plane and from out-of-focus planes. The diameter of the detection pinhole is chosen to be less than or equal to the central maximum of the diffraction-limited spot, i.e., the size of the *Airy disk* (and therefore often expressed in 'Airy units'). Light emerging from points in front of, behind or beside the point of interest at the focus of the objective will not converge at the same spot, and, therefore, only a small fraction of the emitted out-of-focus light will pass through the confocal pinhole (illustrated as dotted and dashed lines in Fig. 2A). As is done in classical epifluorescence, the fluorescence emission is spectrally separated from the reflected and scattered excitation light. Detection is typically achieved with an 'area detector' (i.e., a detector that is not spatially resolved), such as a photomultiplier tube or avalanche photodiode.

This simple confocal geometry produces the 'image' only of a point. One method to obtain a two-dimensional (2-D) image is to move the sample relative to the focused spot in the *xy* plane. For each position, the fluorescence intensity is digitally recorded, and its value assigned to the corresponding *xy* position on the displayed image. Thus, in contrast to the process in wide-field (camera-based) imaging, in confocal imaging, the image is *sequentially* constructed from a two-dimensional (2-D) array of point intensities. 3-D image stacks are achieved by additionally moving the objective with a precision motorized focus.

Modern confocal microscopes move the excitation light beam rather than the sample: a laser beam is expanded to fill the objective's back focal plane (BFP) and its angle of incidence in the BFP is scanned with a pair of galvanometric mirrors or other scanning devices. This arrangement typically requires a high-quality *scan lens* and the classical *tube lens* that (nearly) form a telescope. As a result of beam scanning, a diffraction-limited spot sweeps the focal plane (Fig. 2B; for simplicity, only a single mirror is illustrated). The problem is that, to maintain confocality in the detection pathway, the pinhole must be scanned as well. Therefore, the pinhole (and detector) are usually placed behind the pair or scanners so that the fluorescence collected from that spot traces back the same light path and is 'descanned' before hitting the pinhole. This makes the microscope fairly alignment-sensitive. An interesting recent variant for a confocal microscope based on a nonlinear detection scheme that uses a transmitted pulsed-excitation beam and a virtual pinhole to obtain a confocal transmission image is discussed below [12].

2.4. Nonlinear microscopies

Although they typically also require spot scanning, nonlinear microscopies are based on very different

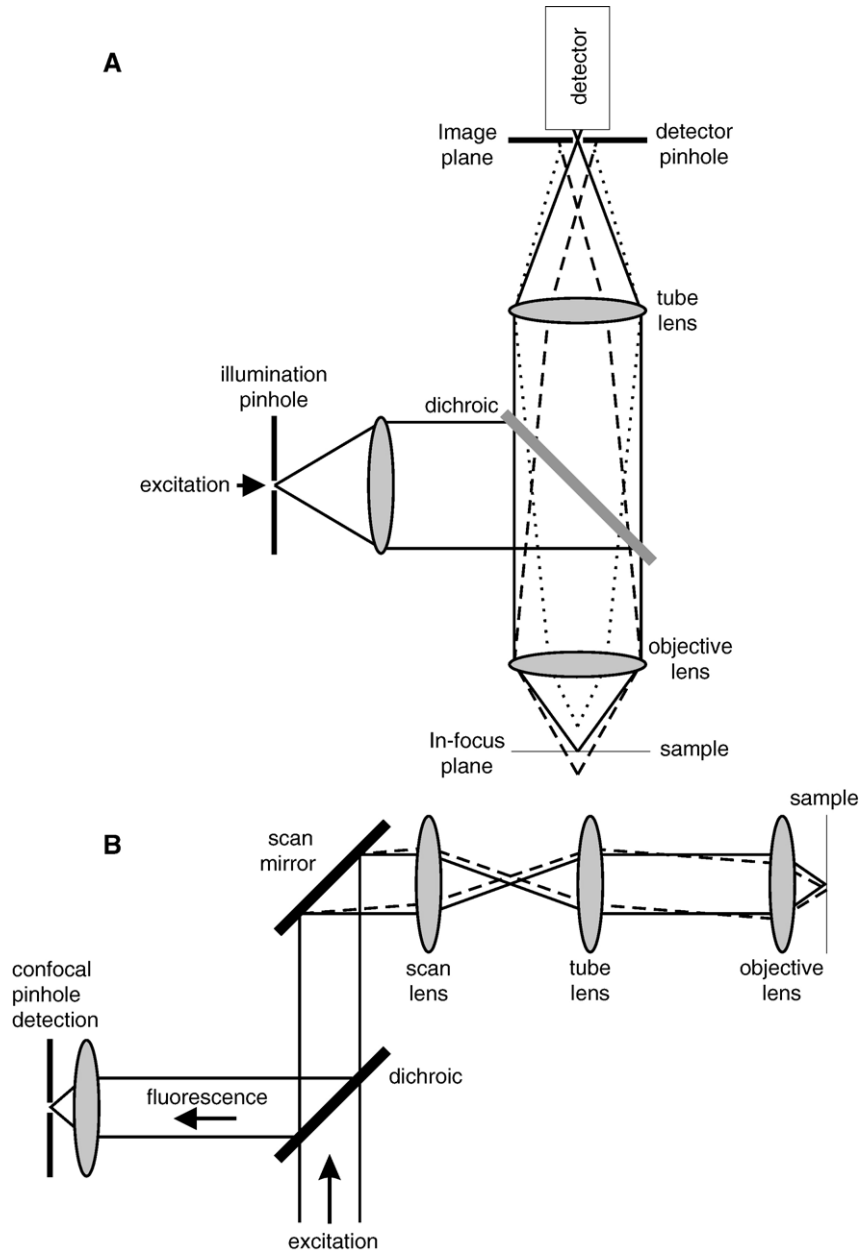

Fig. 2. (A) Confocal detection generates crisper images by the suppression of photons from out-of-focus planes by placing a tiny pinhole in front of the detector. However, also fluorescence emanating from peripheral locations of the focal plane are rejected, so that scanning of the sample relative to the beam is required to form a 2-D image. (B) Sketch of the optical elements in a scanning microscope.

principles. In multi-photon excitation, the excitation wavelength is chosen so that the fluorophores are excited only when absorbing more than one photon (see below). In another method (reversible saturation), the interaction of fluorophores with light of the *emission wavelength* is used to reduce the sample volume that actually fluoresces (see Section 3.9). A very concise and readable survey of the principles of multi-

photon excitation fluorescence microscopy (MPEF) is found in ref. [13]. A compact listing of the instrumentation required is found in the same volume [14].

Two-photon excitation fluorescence (2PEF) refers to the excitation of a fluorophore when two photons arrive within a time window of an attosecond (10^{-18} s) and team up to excite the molecule. Any combination of photons of different energies that sum up to give the energy difference between S_0 and S_2 will do. For practical reasons, two photons of equal wavelength are usually used (Fig. 1B). Once in the excited state, the electron shares the same fate as it would after single-photon excitation (Section 2.1, above). Nonlinear excitation requires extremely high photon flux, typically 10^{20}–10^{30} photons/(cm^{2}s). Hence, under normal daylight or arc-lamp illumination, the probability of two-photon absorption is virtually zero [15]. The experimental demonstration of Maria Göppert-Mayer's prediction of multi-photon excitation had to await the advent of a mode-locked laser that emits photons intermittently in high-intensity bursts rather than in a continuous beam [16]. Although nonlinear optical spectroscopy rapidly expanded from the early 1960s, it was another 30 years before Denk et al. realized the potential of nonlinear fluorescence excitation for laser-scanning microscopy [17].

To attain the high photon flux required for the desired nonlinear effects, pulsed light (instead of continuous-wave illumination) is used. The Ti:sapphire laser that is generally favored generates picoseconds to ~100 fs pulses of high peak power, but at a low repetition rate (~100 MHz, i.e., 10 ns between two pulses) and thus low average power (typically some 10 mW, for laser powers of up to 1 W). In addition, the laser beam is focused to a diffraction-limited volume, using a moderate to high-numerical aperture (NA) microscope objective. By concentrating photons both temporally and spatially, the probability of multi-photon absorption is greatly increased. Furthermore, the two-photon requirement for fluorescence excitation implies that the generated fluorescence will depend on the square of the number of photons per time and cm^2, i.e., the intensity squared (the reason this approach is called "nonlinear"). As a result of focusing the beam, the intensity along the optical axis increases to the focus and then decreases as the distance squared, so that 2PEF rises and then dwindles as the distance raised to the fourth power, confining 2PEF to the immediate vicinity of the focal spot (Fig. 3). The effective 2PEF volume is less than a femtoliter (10^{-15} l–1 μm^3). To obtain optical sections, one can

Fig. 3. An experiment to illustrate the difference between ordinary (single-photon) excitation of fluorescence and two-photon excitation. The cuvette contains a solution of the dye safranin O, which normally emits yellow light when excited by green. The upper lens focuses green (543 nm) light from a continuous-wave (CW) helium-neon laser into the cuvette and produces the expected conical pattern of excitation, fading to the left due the self-absorption in the concentrated dye solution. The lower objective lens focuses a pulsed infrared (1046 nm) beam from a neodymium-YLF laser. One infrared photon alone is not sufficiently energetic to excite fluorescence, so that two photons need to team up and join their energies. Two-photon fluorescence excitation is proportional to the intensity squared, confining fluorescence generation to a small spot in the focal plane where the density of photons is high. This focal volume (arrowed) can be raster-scanned to anywhere in the cuvette thereby creating a point-wise, sequential 3-D representation of fluorescence intensity. (Image credit: Brad Amos/Science Photo Library, London).

scan this excitation spot across the sample, as in confocal laser-scanning microscopy.

As a consequence of nonlinear excitation, 2PEF emission intensities are proportional to the square of the excitation intensity. The maximum fluorescence excitation rate is limited (as in the 1PEF case) by fluorophore ground state depletion (saturation). There are no differences in the 1PEF and 2PEF emission spectra, and emission spectra are independent of excitation wavelength. On the other hand, the 2PEF absorption spectra can substantially differ from their 1PEF counterparts. Although some fluorophores display nonlinear absorption spectra that resemble the 1PEF spectra plotted on an expanded wavelength scale (×2), this is not the general rule. With two-photon excitation, the momenta of the two excitation photons combine to give a higher degree of freedom than is found in single-photon excitation, thereby relaxing the quantum mechanical selection rules. Thus, nonlinearly excitation allows electrons to access excited states like S_2 and S_4, higher than what is accessible with 1PE, resulting in broader 2PEF absorption spectra for many fluorophores.

To compare and quantify 2PEF brightness among different fluorophores, instead of using the product of $\varepsilon\phi$ as is done in the 1PEF case, we define a two-photon action cross-section as $\sigma_{2\omega}\phi$, where $\sigma_{2\omega}$ is the two-photon absorption cross-section and ϕ is (again) the quantum efficiency. For example, rhodamine 6G has a $\sigma_{2\omega}\phi$ of 40 Göppert-Mayer units (GM; 1 GM= 10^{-50} cm^4 s/photon) at 830 nm. The absolute values of 2PEF cross-sections are generally obtained by comparison with 1PEF assuming equal emission quantum efficiencies.

What, then, are the advantages of using a costly and complicated mode-locked laser to generate a small spot of light that is scanned in the same manner as for single-photon laser-scanning confocal microscopy? The main advantage is that excitation occurs only where it is needed–in the focal spot–and all fluorescence comes from this well-defined tiny excitation volume. Table 1 summarizes a number of advantages that directly derive from the nonlinear near-infrared excitation of fluorescence and provides references for further reading.

In view of the already extensive literature on 2PEF imaging in the biological sciences, we focus here on three areas in which multi-photon imaging shows particular advantages over its widely used one-photon optical sectioning counterpart, confocal fluorescence microscopy:

- imaging deep inside scattering tissue
- generation of optical contrast based on nonlinear interactions of light with molecules, not leading to fluorescence—e.g., nonlinear coherent backscattering (higher harmonic generation), coherent anti-Stokes Raman scattering (CARS). We also discuss a version of fluorescence microscopy that uses two pulsed laser beams, one for fluorescence excitation, the other for spatially selective fluorescence deletion, stimulated emission depletion (STED) microscopy.
- multi-color imaging of thin samples, e.g., the near-membrane space in cultured cells, biofilms or biochips.We also briefly review new developments of specifically tailored 2PEF dyes, and some particularly notable applications of nonlinear microscopy.

3. Recent developments in nonlinear imaging

Although introduced more than 15 years ago, multi-photon imaging is still a rapidly evolving technique. Examples of the continuing advances include the design of new (both more rapid and more flexible) 2PEF geometries, the ongoing miniaturization of 2PEF devices and the expansion in availability of newly synthesized fluorophores with large 2PEF cross-sections.

Perhaps the observation that most emphasizes the relative youth of the field is that the leading laboratories in the field continue to use home-built instrumentation rather than commercially available instruments. While part of the appeal to using home-built systems is that a ‘stripped-down’ microscope built on a simple optical-rail-based system allows free access to all optical components and facilitates their alignment, a more important reason to use home-built systems is that, until recently, most commercial systems were single-photon confocal systems modified for multi-photon imaging applications. As will be clear in the next section, adapting a single-photon confocal system for multi-photon imaging is far from ideal, due to the less efficient collection of emitted fluorescent photons, related to the use of the pinhole and descanned detection.

In the meantime, a fair number of ‘*how to build a two-photon microscope*’ manuals have been published

Table 1
Advantages of nonlinear fluorescence excitation over confocal detection

Problem	Multi-photon excitation	References
Requirement for multiple lasers/illumination sources for multi-color fluorescence imaging	Multi-photon excitation at a single wavelength stimulates fluorescence in fluorophores, having a broad range of 1PEF excitation maxima, because 2PEF absorption spectra are much broader than 1PEF absorption spectra. This is due to the relaxation of the quantum mechanical rules that results from the higher degree of freedom associated with the sum of the momenta of two photons. Also, 2PEF microscopy holds the potential to record full fluorescence spectra (due to the excitation removed to the IR), e.g., for linear unmixing of overlapping fluorophores.	[51,112]
Loss of contrast by scattering of excitation photons	Infrared light used in 2PEF is subject to less absorption and scattering than UV or visible light so that excitation penetrates more deeply into a sample. Those photons that do get scattered are to dilute to produce 2PEF. They are lost for excitation, but do not do further harm to image contrast. At very large imaging depth, light photons traveling at the greatest angles to the optical axis are filtered out, due to the longer path traveled by photons (and higher probability of being scattered), so that the effective NA for 2PEF excitation is reduced and the excitation less efficient.	[17]
Loss of resolution due to out-of-focus fluorescence excitation	Multi-photon excitation confines fluorescence excitation to a small volume at the focus of the objective. Photon flux is insufficient in out-of-focus planes to excite fluorescence, except for extremely high laser power (see below).	[22,25]
Photobleaching and photodamage throughout the sample	Photobleaching and photodamage are limited to the zone of 2PEF and do not occur above or beyond the focus. However, they are highly nonlinear.	[24]
Light collection efficiency	Since 2PEF is localized to a point, no confocal pinhole is needed. No requirement for de-scanning, less alignment sensitive. All fluorescence constitutes useful signal.	[22,27,28]
Limited depth penetration	As noted above, IR photons travel deeper into tissue with less scattering and absorption. The loss that does occur can be compensated for by increasing laser power. Laser power, however, cannot be raised indefinitely, both due to instrument power limitations and tissue damage. Recent findings indicate a fundamental limit that stems from (diffuse) surface fluorescence excitation, which produces a surface-derived signal comparable in magnitude to the small signal coming from the 2PEF spot deep in tissue. This diffuse signal invalidates the assumption behind 2PEF imaging that all fluorescence originates from the focus, rises the background and lowers contrast.	[23,27]

[14,18–20], and the availability of the software code that permits controlling the galvanometers and image acquisition from the Svoboda lab [21] has largely contributed to expand the use of this (former) 'expert technique'.

3.1. Linking morphology and function in deep-tissue imaging

2PEF imaging is particularly well suited for deep-tissue imaging. There are two major reasons for this advantage: (1) The longer-wavelength (infrared) light used is much less subject to absorption and scattering than the visible wavelength light used in single-photon confocal imaging (the degree of scattering scales approximately with the wavelength raised to the fourth power, $\sim\lambda^{4,2}$); and (2) the light collection pathway can be designed to be more efficient than in single-photon confocal microscopy.

Nonlinear excitation at depth. Although infrared light is less susceptible to scattering and absorption than visible light, infrared excitation photons are nevertheless lost exponentially with imaging depth z. In fact, due to the two-photon requirement, the generated

[2] Light scattering by particles of about the same size as the wavelength λ is described by Mie theory, whereas Rayleigh scattering applies to particles much smaller than λ. Rayleigh scattering describes, for example, the well-known phenomenon of the scattering of sunlight to form the blue sky and is dependent on λ^{-4}.

2PEF decays even faster—proportional to $\exp(2z/l'_s)$, where l'_s is the reduced scattering length.

However, increasing the incident laser power may be used to compensate for this decay in 2PEF, an advantage over 1PEF, for which increasing laser power would lead rapidly to increased out-of-focus fluorescence, due to excited fluorescence by scattered photons. In the 2PEF case, scattered photons are too low in energy and dilute to excite out-of-focus fluorescence.

With this 'brute force' approach, imaging can be achieved to a maximum depth of about 600 μm in rat or mouse brain tissue [22]. For greater depths, redistributing the same average power into higher peak power pulses, at the expense of lower pulse repetition rate, can be used to maintain a high level of fluorescence excitation [22], permitting 'ultradeep' 2PEF recordings of neurons and blood vessels down to a millimeter into mouse brain tissue [23]. This is because 2PEF power (i.e., fluorescence intensity) is proportional to $\bar{P}_0^2/(r\tau)$, where $\bar{P}_0$ is the average laser power in focus, r is the laser repetition rate and τ is its pulse duration. However, at extremely high pulse peak power, the sample can become damaged [24] or the probability of fluorescence excitation per pulse can begin to saturate. Also, the laser intensity at the tissue surface can attain levels that lead to unfocussed bulk 2PEF generation and consequent loss of contrast.

Light collection rather than imaging. 2PEF imaging relies on systematic scanning of a near-diffraction-limited excitation volume throughout an image plane in the specimen. At each scanner position, all fluorescence originates from a single multi-photon excitation volume. Thus, every fluorescence photon exiting the sample provides useful information about a single location in the sample and should ideally be collected, even if scattering occurs along the collection pathway. This recognition has four important consequences on the design of an optimal 2PEF imaging system.

First, when imaging samples that allow access from either side (e.g., cultured cells, brain slices or thin tissue explants), fluorescence photons should be collected both in the upright/backward (epi-) direction and in the forward/transmitted direction, so as to increase the *effective NA* of the collection optics. Second, a detection pinhole is not needed, and is even detrimental, since, as noted above, all emitted fluorescence photons should be collected, including photons that due to scattering would not converge and pass through a confocal pinhole. Third, for optimal photon collection, detectors should be located as close to the fluorescence source as possible, to reduce loss of scattered fluorescence photons. Indeed, use of non-descanned 'proximity' detectors is better for high-sensitivity 2PEF detection than threading the fluorescence light back through the scanning pathway, as is normally done for single-photon laser-scanning confocal microscopy [25–27]. Fourth, the requirement for high photon collection efficiency rather than high-resolution imaging *per se* implies that the microscope collection optics should contain a minimum of intermediate optical components and those present should be large numerical and clear aperture. For the purpose of focusing the laser beam to a diffraction-limited spot, the microscope objective should still be moderate NA (~0.8), but for purposes of photon collection it should also have as wide a field-of-view as possible, and thus relatively low magnification [27] so as to collect a maximum of scattered photons. When the condenser is used for fluorescence collection as well [18], large NA and field-of-view should be favored over high aberration correction. When whole-field detection is optimized, following the guidelines suggested above, the detection efficiency does not decrease significantly with depth [27,28], so that photon collection remains possible until fluorescence absorption in tissue becomes significant.

3.2. Rapid, random-access scanning

Scanning the laser beam across the specimen plane in two orthogonal directions (*xy*) is typically performed with a pair of small mirrors mounted on fast galvanometers. Galvanometric mirrors provide fast (1 ms) accurate scans of large amplitude (~± 10°). The duration and full length of the line scanned in the specimen plane depend on the speed and full angle swing of the scan. In contrast to the fixed dimensions of CCD cameras, where the number of pixels is set by the hardware architecture, the number of pixels into which the scanned line is partitioned is arbitrary and will depend on the acquisition rate (time per pixel). Typically, the dwell time per pixel is on the order of a few microseconds and the extent covered by each 'pixel' chosen to be no smaller than the size of the 2PEF volume.

Galvanometric scanners are convenient for acquiring full images or not-too-small image subregions.

Image acquisition is serial, i.e., pixel by pixel (x-scan with a sawtooth command voltage), one line after the other (one 'pixel' y-'scan' (i.e., line feed) after completion of each x line and flyback). Bidirectional x scanning, which is implemented on some commercial 2PEF machines, can speed up the acquisition rate and reduce dead time. However, true video rate scanning requires resonant galvanometers (i.e., galvanometers that are driven at their resonance frequency, but the time per pixel will be unevenly distributed. Alternatives include polygonal spinning mirrors, multiple beam splitting [29] or acousto-optic deflectors [30]. To monitor rapid physiological processes occurring on time-scales of a few milliseconds, line- or point-scans can be used, as long as a complete image is not required. In comparison with mirror-based approaches, acousto-optic deflectors (AODs) have the advantage of rapid, freely addressable point-wise random-access scanning [31]. For example, multi-unit recordings of action-potential evoked calcium transients in the somata of pyramidal neurons have been recently demonstrated [32]. In this case, instead of a full image, a temporal sequence of isolated spots is repeatedly scanned. An acousto-optic modulator precompensates the large distortions of femtosecond pulses in the AOD-based scanner [33].

3.3. Fiber delivery of ultrashort nonlinear pulses

Many 2PEF applications benefit from the separation of the fairly bulky laser equipment from the microscope. For example, one laser could be shared among different scanheads. Also, one high-power laser could, in principle, provide light for multiple microscopes.

To dissociate the microscope from the light source, the excitation light can be delivered through an optical fiber (see, e.g., [34–36] for review). However, femtosecond laser pulses broaden in optical fibers because of temporal dispersion and – at high laser powers used for deep-tissue imaging – because of nonlinear self phase modulation. As dispersion is already a concern for the limited number of optical elements present in the imaging system (lenses, objective), minimizing the additional dispersion introduced by an optical fiber is essential. The 2PEF power (i.e., fluorescence intensity) is proportional to $\bar{P}_0^2/(r\tau)$ (see above), so that pulse broadening (increase in τ) will reduce the amount of fluorescence and must be kept to a minimum. Traditionally, pulse dispersion is 'pre-compensated' by passing the beam through a pair of dispersive elements–gratings or prisms–in a double-pass configuration. However, at high laser powers, nonlinear interactions of the pulse with the fiber core become dominant, so that compensation is very poor. Although special large-core fibers [35], and spectral pulse precompensation [37] offer at least a partial remedy to the problem of pulse distortion, only the recent introduction of microstructured photonic-crystal hollow-core fibers [38,39] has permitted the distortion-free delivery of high-energy femtosecond pulses.

3.4. Two-photon fiberscopes for imaging freely moving animals

A direct consequence of the ability to propagate ultrashort pulses through optical fibers is that the microscope and laser equipment no longer need to be located together on a large optical table [4]. A number of recent studies has taken advantage of this advance, abandoning the conventional microscope body in favor of a miniaturized 2PEF scanning microscope, light enough to be carried by an adult rat and glued on its head with dental cement. In the original demonstration [40], laser pulses from a conventional Ti:sapphire femtosecond-pulsed laser were propagated through an optical fiber, collimated by a small lens and focused through a miniature water-immersion objective. Fluorescence was either collected by a small photomultiplier or the collected fluorescence was fed back through a large-core fiber using a remote detector. Image formation was achieved by resonantly scanning the end of the (thin) optical fiber with a piezoelectric vibrator. By breaking the symmetry through stiffening the fiber in one direction only, a second resonance was generated which could be used to perform an area scan with a Lissajous pattern. A more recent version of the device even includes a miniature translator for moving the objective in z direction [35].

In vivo recordings have traditionally been limited to anesthetized, head-restrained animals held in a stereotactic apparatus. Although the fiberscope holds the promise of deep optical recordings in awake behaving animals, one current limitation when using the fiberscope in awake animals is that abrupt

movements of the head result in artifacts due to movement of the brain relative to the skull. Another challenge is finding methods for targeting and specific delivery of fluorophores to large imaging depths in a live animal. Transgenic mice expressing fluorescent protein labels in defined cell populations are an attractive solution to this problem; however, the fiberscope apparatus will have to be further miniaturized for mice, or investigators will have to develop transgenic rats.

In a related application, 2PEF *in vivo* imaging has entered the domain of endoscopy. Here, instead of the bulky objective and intermediate optics, a fiber-coupled gradient-index (GRIN) lens is used to provide a compact and miniature endoscopic microscope head [41–43]. GRIN lenses, instead of using curved shaped surfaces, have only planar optical surfaces. Their performance depends on a continuous change of the refractive index within the lens material. The light rays are continuously bent within the lens until they are focused to a spot. Focusing is achieved by adjusting the gap between the fiber coupler and the entrance face of the GRIN lens. The modalities of optimal coupling of GRIN lenses to single-mode optical fibers have been characterized [44]. Spectrally resolved recording of endogenous fluorescence by means of 2PEF endoscopy could prove to be an important diagnostic tool, obviating the need for surgical biopsy in both research and clinical applications.

3.5. Chemical uncaging, ablation, histology and light-induced permeabilization

An important application of localized two-photon excitation is the photolysis of photolabile or photoactivable 'caged' compounds in a variant of two-photon microscopy known as chemical uncaging microscopy. In this application, a cellular response linked to the locally released molecule is monitored, rather than fluorescence [26]. The responses can be mapped in pseudocolor in an image to present the spatial distribution of the amplitudes of the cell's response to the uncaged substance. Compared to a 2PEF image, these maps are spatially somewhat broadened due to the diffusion of the caged compound, depending on the nature of the sampled response. For example, to study functional synaptic connectivity and to identify the principles underlying the construction of the cortical columnar architecture, the Svoboda lab has used quantitative two-photon glutamate uncaging to measure the strength of excitatory projections from layers 4 and 5A to layer 2/3 pyramidal cells in barrel- and septum-related columns [45,46].

Another very interesting application of 2PEF imaging has been to combine high-resolution histology and physiological recordings. Tsai et al. used the nonlinear interaction of light with brain tissue first to image (at low to moderate power) fluorescently labeled cells at progressively deeper levels until fluorescence contrast was lost (cf. Section 3.1) and then to ablate (at high-power) tissue sections [47]. Cuts were accomplished with 1 to 10 μJ pulses to ablate tissue with micron precision. The study demonstrated the use of femtosecond laser pulses to iteratively cut and image fixed as well as fresh tissue.

With the goal of large-scale histological reconstructions of previously imaged live tissue, the Denk lab has combined automated block-face imaging with serial sectioning inside the vacuum chamber of a scanning electron microscope [48]. In their approach, electron microscopy follows 2PEF imaging. Their technique generates contrast from backscattered electrons rather than the heavy-metal staining of tissue that are routine for transmission electron microscopy. Low-vacuum conditions prevent charging of the uncoated block face. The resolution is sufficient to trace even the thinnest axons and to identify synapses previously imaged in living state with 2PEF microscopy. This opens the possibility of automatically obtaining the electron-microscope-level 3-D datasets needed to completely reconstruct the connectivity of neuronal circuits. Together, both approaches present a powerful means to automate the three-dimensional histological analysis of tissue with important implications for screening large quantities tissue sections, of, e.g., pathologically altered and control tissue.

On a much smaller scale, two-photon absorption was used to locally photoinduce the flip-flop of stilbazolium markers in model lipid bilayer membranes [49]. Photoisomerization provoked a significant increase in the *cis*-marker population whose rate of redistribution between the inner and outer membrane leaflet ('flip-flop') was > 1000× faster than that for *trans*-markers. Interestingly, the flip-flop of the fluorophore transiently perforates the membrane, opening the possibility of controlled and localized

depolarization of the membrane potential or micro-scale drug delivery in deep tissue.

3.6. New fluorophores

While important progress has been made in tailoring 2PEF instrumentation to specific applications, until recently, the optimization and synthesis of dedicated "two-photon fluorophores" (see Section 2.4) has received much less attention. In fact, many commercially available fluorescent probes that have been used in 2PEF imaging exhibit relatively low two-photon absorption cross-section values in the tuning range of the Ti:sapphire laser [50]. Furthermore, many available fluorophores are plagued with low fluorescence quantum yield and/or high two-photon absorption photoinstability (i.e., high photobleaching). The most complete compilation of 2PEF absorption spectra and action cross-sections comes from the seminal work of Chris Xu et al. [51].

More recently, different laboratories have prepared fluorophores tailored for multi-photon imaging. Rather than being derived from the classical fluorescein, rhodamine or tetramethylrhodamine backbone, these new fluorophores are based on a fluorene ring system [52] or organoboron compounds (donor-pi-acceptor (D-π-A) type compounds), with a trivalent boron, protected by two mesityl groups, as acceptor, and with various typical donors and different π-conjugated bridges [53]. Although these dyes predominantly fluoresce in the blue-green region of the visible spectrum, orange-red fluorescing 2,1,3-benzothiadiazole (BTD)-based D-π-A-π-D-type fluorophores have been recently described [54]. A different strategy uses novel octupolar propeller-shaped fluorophores derived from the symmetrical functionalization of a triphenylamine core with strong acceptor peripheral groups via phenylene–ethynylene to obtain high fluorescence quantum yields, very large 2PEF cross-sections in the red–NIR region, and suitable photostability [55] or use click chemistry to combine a broad, very high two-photon absorption in the NIR region. Due to the marked dependence of their emission spectra on solvent polarity, these dyes have been proposed as model probes for two-photon sensing of the chemical environment [56,57].

Similar efforts are being undertaken with respect to synthesizing photosensitive 'caged' compounds with large two-photon absorption cross-sections [58–60] as well as fluorescent dyes that, in addition to exhibiting a large 2PEF cross-section, possess a large second harmonic generation cross-section (see Section 3.7).

3.7. Higher harmonic generation

Focusing a pulsed laser beam into a sample can generate harmonic up-conversion, as well as multi-photon excited fluorescence. Higher harmonic generation (i.e., frequency doubling or tripling) does not arise from absorption but from hyper Rayleigh scattering (Fig. 4A). Although the nonlinear optical effect known as second harmonic generation (SHG) has been recognized since the early days of laser physics and was demonstrated through a microscope almost 30 years ago [61,62], the use of SHG and its three-photon variant, third harmonic generation (Fig. 4B), for three-dimensional image contrast is fairly recent (see [7,63,64] for reviews). Both imaging of nonlinear fluorescence and of nonlinearly backscattered light can provide similar resolution and, for sufficiently high dye labeling, give comparable signal levels, so that only small modifications are required to equip a standard laser-scanning 2PEF microscope for harmonic generation imaging microscopy [65,66] allowing them to be combined in a single scanning microscope. Because

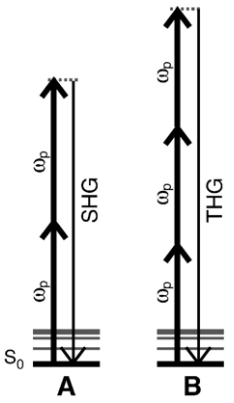

Fig. 4. Jablonski diagram of second (A) and third harmonic generation (B). Higher harmonic generation does not require actual absorption but is based on the nonlinear scattering of two low-energy photons that produce one frequency-doubled photon. They also differ from multi-photon absorption in that they are phase-preserving, i.e., coherent, which causes a nonlinear dependence on the molecule density, directed emission lobes and cancellation.

higher harmonic generation is a coherent process, most of the signal propagates in the same direction as the incident laser beam. The exact ratio of forward (transmitted) and backward (epi) signal depends on the sample characteristics.

However, being a coherent superposition of individual molecular emissions, harmonic contrast generation differs fundamentally from fluorescence in that it produces directed radiation patterns that are highly sensitive to phase, rather than an isotropic glow in all directions (like fluorescence). This property raises the issue of directional detection but also makes SHG imaging microscopy unique in allowing one to probe molecular orientation and alignment. Higher harmonic generation is a consequence of the *nonlinear polarizability* P of a material, $P=\chi^{(1)}E+\chi^{(2)}E\otimes E+\chi^{(3)}E\otimes E\otimes E+\ldots$ The familiar phenomena of absorption and reflection correspond to its linear term, and under usual illumination conditions, the higher-order terms are neglected. Arising from the second-order term, as do sum and difference frequency generation as well as hyper-Rayleigh scattering, SHG requires higher illumination intensities. Multi-photon absorption, THG and coherent anti-Stokes Raman scattering (CARS, see Section 3.8) are third-order processes.

The second-order (SHG-) term of the nonlinear hyperpolarizability is proportional to the square of electromagnetic field, with $\chi^{(2)}$ as a proportionality constant. This second-order nonlinear susceptibility $\chi^{(2)}$ is a *bulk* material property that relates to the *molecular* hyperpolarizability, $\langle\beta\rangle=\chi^{(2)}/N_s$, where N_s is the density of dye molecules and the brackets denote an orientational average. Thus, $\langle\beta\rangle$ is maximal for parallely aligned molecular dipoles (e.g., membrane resident dyes) and zero for antiparallely oriented molecules, the contributions of which interfere destructively due to their phase shift. In bulk solution, one can always find a pair of molecules that are antiparallel and cancel their respective contributions. This makes clear, why SHG requires a polarizable material with noncentrosymmetric symmetry. Compared to the previously introduced two-photon absorption cross-section, SHG cross-sections are typically much smaller, but as the signal from coherent sources sums up $\propto N_s^2$ (compared to $\propto N_s$ in the case of the (incoherent) fluorescence emission), a high enough density of SHG labels can, in part, compensate for the small signal from individual molecules.

Recent studies of the three-dimensional *in vivo* structures of well-ordered protein assemblies, such as lipid membranes [65], collagen [67,68], microtubules [69] and muscle myosin [70] are beginning to establish SHG imaging as a nondestructive microscopy technique that holds promise for both basic research and clinical pathology. In addition, SHG signals from certain membrane-bound dyes have been shown to be highly sensitive to membrane potential [71–76]. THG, in turn, depends much less on molecular orientation [77], is comparable to 3PEF [78], and has been shown to provide label-free images of lipid bodies in hepatocytes [79].

Finally, Yang and Mertz presented an interesting transmission nonlinear microscopy based on SHG contrast [12]. Using a standard 2PEF microscope, they collected through a second objective and refocused the transmitted IR light onto a nonlinear crystal. This crystal causes a frequency doubling via SHG and emits SHG only at the point where the focused light impinges on the crystal. The transmitted intensity can be used to generate a transmitted confocal contrast. The local SHG signal therein acts as a 'virtual pinhole', which is automatically aligned with the scanned beam. This configuration is otherwise difficult to achieve, because one would need two synchronized pairs of scanners.

3.8. Coherent anti-Stokes Raman scattering (CARS)

In the 1920s, Raman noticed that light incident on a variety of surfaces is sometimes scattered with wavelengths different from the incident light. There are two types of scattering occur when visible light is incident on molecules: elastic and inelastic. Elastic scattering occurs when the scattering light has the same energy (and thus wavelength) as the incident light; this process is termed Raleigh scattering. The much less frequent event of inelastic scattering (termed Raman scattering) corresponds to the case where the energy of the scattered photon is different from the incident light. The difference in energy occurs because the molecule changes its vibrational state during the scattering process. Raman scattering is based on exciting chemical bonds with visible light. As for higher harmonic generation, it requires the induction of a (in general) nonlinear polarizability P (see above). Unlike fluorescence or higher harmonics, vibrational spectra contain a

multitude of molecular signatures due to the excitation of specific chemical bonds. In the context of biological imaging, these can be used for generating contrast without exogenous labels. Raman scattering involves no electronic absorption and molecular excitation. The scattering process occurs via a "virtual state" which is generally not an electronically excited state of the system. However, the Raman signal is significantly enhanced if the incident light is resonant with an energy level of the molecule. This is called resonant Raman scattering (RRS) and can be many orders of magnitude larger than its ordinary nonresonant analog. Unfortunately, RRS overlaps with the fluorescence and the two signals can be awkward to separate.

Since the advent of the laser, which offers monochromatic light, RRS has been extensively studied. The molecule that scatters the incident light can either end up in a higher vibrational state in which case the scattered photon is red shifted compared to the incident light. This type of light scattering is termed "Stokes scattering", in reference to the red-shift of the scattered photon (Fig. 5A). Alternatively, the molecule can end up in an energy state lower than its initial state via the emission of a blue-shifted photon ("anti-Stokes scattering") (Fig. 5B). Anti-Stokes scattering requires the molecule to start out in a vibrationally excited state.

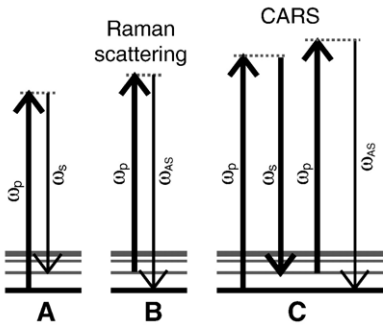

Fig. 5. Jablonski diagram of (A) Stokes Raman scattering, (B) anti-Stokes Raman scattering and (C) coherent anti-Stokes Raman scattering (CARS). CARS involves a pump beam (upward arrows with frequency ω_p), a Stokes beam (ω_s) and a signal at the anti-Stokes frequency $2\omega_p-\omega_s$ generated in the phase- matching direction. CARS is sensitive to molecular vibration states and can be used to detect the presence of specific types of chemical bonds. Contrast is generated when the difference between pump and Stokes beams is tuned to be resonant with a Raman-active vibration. Incident beams are shown with thicker lines while the detected signal is shown with a thin line.

At room temperature, only low lying vibrations ($< 200\ cm^{-1}$) will be appreciably excited, and hence only Stokes scattering is typically probed.

Raman scattering has been used to acquire microscopic images, albeit at limited sensitivity and resolution [80]. Also, autofluorescence excited by the visible incident light will mask the faint Raman signals [81] and further reduce image contrast. Nevertheless, Raman imaging has some distinctive advantages over fluorescence techniques and provides a direct way of imaging unstained live cells. Unlike fluorescence, which generally relies on exogenous labels to acquire its specificity, Raman scattering directly provides chemical selectivity due to the resonant frequency of the excited molecular bond.

With the advent of lasers in the 1960s, it was realized that Raman signals could be enhanced based on the nonlinear mixing of optical waves. Stronger signals can be measured with coherent anti-Stokes Raman scattering (CARS). In contrast to the single-beam Raman signals discussed above, CARS is a nonlinear Raman technique that involves multiple laser beams incident with the sample. CARS signals require a pump beam at frequency ω_p and a second Stokes beam at frequency ω_s interact with a sample to generate a new anti-Stokes signal at a different frequency and direction from the applied laser pulses (Fig. 5C). When the beat frequency between the pump and Stokes matches the frequency of a particular Raman- active molecular vibration, the vibrations are coherently driven, which results in an enhanced anti-Stokes signal that can be used to image different vibrations in probed samples. CARS possesses a higher sensitivity than Raman microscopy because the coherent CARS radiations produce a large and directional signal [82–84]. This leads to a lower average excitation power and consequently less photodamage to cells. Moreover, the nonlinear excitation intensity dependence of CARS provides inherent 3-D sectioning capability, similar to 2PEF microscopy. CARS imaging can also be performed on non-tagged samples without the introduction of bulky non-native fluorophores.

3.9. Stimulated emission depletion (STED) microscopy

The concept of stimulated emission depletion (STED) microscopy was introduced a decade ago by

Hell et al. and Schrader et al. [85,86] (reviewed in [87,88]). STED provides nanometer resolution in a far-field detection geometry [89]. The principle that underlies this variant of nonlinear microscopy is to use two precisely timed and successive light pulses, one to create an excitation volume and the other (the so-called "STED beam") to pare down the region that fluoresces by illuminating the excited fluorescent molecules with short-lived, donut-shaped depletion beam that drives (depletes) the excited states of the fluorophores to the ground state, sparing only the central donut "hole". The trick here is to use a depletion beam that is intense around the focal spot, but dark in the center. This can be accomplished by the use of an optical phase plate that produces destructive interference at the center of the focal spot. The only volume left with fluorescent molecules is the hole of the donut. The excitation beam and the STED beam are of different wavelengths, the former appropriate for excitation, while the latter has the same wavelength as the fluorescence.

Conceptually, STED is based upon an early discovery of Einstein. It had been known for a long time that atoms and molecules could absorb light of one wavelength and then re-emit light of a different wavelength. In 1917, Einstein found that light could also stimulate atoms or molecules to emit light of the same wavelength, polarization and direction of propagation as the incident light. Stimulated emission forces excited molecules into an upper vibrational level of the ground state, whose ultrafast vibrational decay prevents re-excitation by the same beam [90].

Box 1

Total internal reflection fluorescence microscopy (TIRFM)

Also called evanescent field microscopy, TIRF microscopy is a fluorescence imaging technique using near-field excitation and wide-field fluorescence detection to obtain images of surface-proximal thin optical sections [109]. TIRF derives its optical sectioning capability from the total internal reflection of light and generation of an evanescent field at a dielectric interface. Therefore, in contrast to point-scanning optical sectioning techniques, TIRFM imaging is inherently confined to the cell–substrate contact region. Unlike 2PEF scanning microscopy, it does not require beam scanning to form an image of a 2-D sample.

Light hitting a dielectric interface is partially reflected and refracted. *Snell's law* specifies the direction of propagated light; the transmitted and reflected intensities are governed by the *Fresnel coefficients for transmission and reflection*, respectively, which are polarization-dependent and also depend on the angle of incidence of light at the interface, θ. When θ exceeds a *critical angle* $\theta_c = \arcsin(n^1/n^3)$, where n^1 and n^3 are the refractive indices of the liquid and glass coverslip, an evanescent field is created in the rarer optical medium, the intensity of which decays exponentially in the direction of the surface normal. Its depth is given by $d = (\lambda_0/4\pi n_3)(\sin^2\theta - \sin^2\theta_c)$. Although, notably in the case of 'through-the-objective TIRF' [110], deviations from this simple monoexponential behavior are observed [100,111], the rapidly decaying evanescent field creates an optical section that is thinner (100–300 nm) than the sections that can be achieved by either multi-photon imaging or standard laser-scanning pinhole confocal microscopy. Fluorophores located within the penetration depth of the evanescent wave are selectively excited and appear with high contrast against a dark background.

The evanescent wave can be generated through different arrangements. The two principal approaches involve directing light through a prism or through a high-NA ($NA > n_{sample}$) microscope objective—the so-called 'prismless' approach. Fig. 6A and B illustrates two popular choices of how to use a prism to direct a laser beam such that it is reflected at the glass/water interface. Fig. 6C shows the corresponding arrangement for 'through-the-objective' TIRF, in which light is restricted to the marginal rays in a high-NA objective ($NA > n_1$) that intercept the reflecting interface at a supercritical angle.

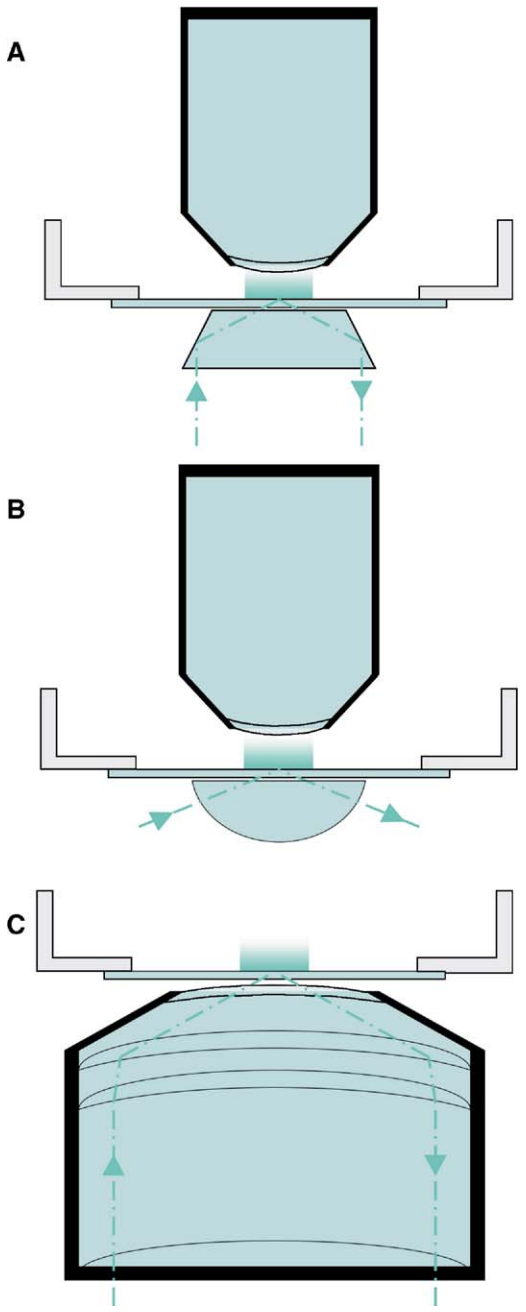

Fig. 6. Popular setups for TIRF microscopy. A and B show examples of arrangements where total internal reflection is obtained by the so-called prism approach using a trapezoidal and hemicylindrical prism, respectively. Panel C illustrates the 'through-the-objective' or 'prismless' approach.

After the STED beam has passed through the focal volume, the majority of molecules not having undergone stimulated emission are still in an excited state and will fluoresce, as the fluorescence lifetime is an order of magnitude longer than the STED pulse duration [89]. Stimulated emission is also the basic process in the laser. For appreciable stimulated emission (i.e., depopulation of the excited state) to occur, lasing requires a population inversion, i.e., a more populated excited than ground state, which is achieved by "pumping" the lasing medium electrically or optically. In as much as resolution in STED images does not depend on diffraction but only on the attainable saturation level, i.e., the STED beam intensity distribution, the focal spot can, in principle, shaped down to a volume of molecular dimensions.

In practice, STED imaging with a resolution of ~30–40 nm, i.e., ~λ/20 to 25 has been demonstrated [91–93]. Also, combined with spectral detection of time-resolved fluorescence, STED can circumvent orientational averaging constraints and spontaneous emission selection rules inherent in all conventional techniques [94]. The technique, although still in its infancy, is already producing impressive results, e.g., in the studying the organization of the presynaptic active zone at the nanoscale [95–97] and will certainly open a view onto the nanoscale world which until now was obscured by diffraction.

3.10. Large-area (non-scanning) two-photon excitation

2PEF microscopy is commonly associated with high-resolution, 3-D sectioning capabilities, large depth penetration and localized photobleaching. Therefore, it lends itself in a natural way to live-cell studies in deep tissue sections (see above). However, the requirements to scan the 2PEF excitation spot to construct 2-D images and to use expensive bulky femtosecond-pulsed lasers have long been considered major drawbacks in pharmaceutical screening applications where a large number of samples have to be analyzed in parallel.

It has recently been shown that when a femtosecond-pulsed infrared beam is reflected at an appropriate interface, conditions may allow for generation of 'macroscopic' evanescent-field two-photon fluorescence excitation [98–100]. In this case, the 2PEF

volume is confined by both the nonlinearity of the multi-photon process and the spatial inhomogeneity of the evanescent field (see Box 1 for details). Restriction of the 2PEF volume to the near-interfacial region defined by the evanescent wave (EW) permits planar 2PEF over a micrometer-sized surface area without the necessity for beam scanning [100]. The illuminated area can be extended and shaped, e.g., for multi-spot plate reading, by the use of resonant waveguide structures [101–103]. An important advantage for creating the conditions of planar 2PEF derives from the local-field enhancement of the evanescent field. The effective space constant of EW 2PEF is roughly equal with EW 1PEF, as the square dependence of the generated fluorescence on the incident laser intensity compensates for the larger penetration depth due to the infrared excitation.

Nonlinear EW excitation has been employed for nonlinear spectroscopy of sodium atoms at a gas/solid boundary [104], for analytical chemistry applications [98] and two-photon pattern photobleaching [105] and EW excited second harmonic generation (SHEW) [113, 114]. The absence of scattered excitation results in a low background (high contrast) and enables simultaneous multi-color fluorescence excitation in a plate reader system. Thus, nonlinear evanescent-field excitation may offer an attractive approach for quantitative single-molecule observation and ultrasensitive screening assays. Another variant of 2PEF TIRFM uses focused evanescent fields in a scanning-type geometry to confine excitation to an attoliter volume [106,107]. The current status, technical requirements and potential of this emerging field of thin-sample 2PEF microscopies have been recently surveyed [108].

4. Summary and conclusions

In summary, we have reviewed the basic principles underlying the nonlinear imaging, and we have surveyed a number of the promising new developments in the field. Nonlinear imaging is maturing from an area restricted to experts bred in physics and biophysics labs into an imaging modality that is increasingly available to many labs. The wider accessibility has been aided by the commercialization of smaller, rugged and less expensive (yet generally less powerful) turn-key femtosecond-pulsed lasers. Multi-photon fluorescence imaging enables fluorescence imaging in tissue at depths of up to a millimeter. CARS and THG, as well as–to a lesser degree–SHG are capable of generating high-contrast images from endogenous biomolecules. Miniaturization of the 2PEF apparatus promises to open up the field to imaging tissues in freely moving animals. The introduction of STED microscopy promises to bring molecular-dimension resolution to optical microscopy. Finally, 2PEF-EW microscopy should make it possible to perform rapid, multispectral imaging in thin films, which should be useful in large-scale screening applications.

Acknowledgements

Work by M.O. lab related to the subject of this review was supported by the Alexander-von-Humboldt Foundation, the Centre National de la Recherche Scientifique (CNRS), the Insitut National de la Santé et de la Recherche Médicale (INSERM) as well as the French Ministry of Research and Technology (*action concertée incitative "jeune chercheur"*). The RHC laboratory is supported by the NIH-NIDDK, the American Heart Association, the Human Frontiers Science Program and a generous gift of the family of Barbara Rose Smith. DM is supported by a fellowship from the Danish Natural Science Council.

References

[1] P. Curley, A. Ferguson, J. White, W. Amos, Application of a femtosecond self-sustaining modelocked Ti:sapphire laser the field of laser scanning confocal microscopy, Opt. Quantum Electron. 24 (1992) 851–855.
[2] K.W. Dunn, P.A. Young, Principles of multiphoton microscopy, Nephron Exp. Nephrol. 103 (2006) e33–e40.
[3] F. Helmchen, W. Denk, Deep tissue two-photon microscopy, Nat. Methods 2 (2005) 932–940.
[4] B.A. Flusberg, E.D. Cocker, W. Piyawattanametha, J.C. Jung, E.L. Cheung, S.M. J, Fiber-optic fluorescence imaging, Nat. Methods 2 (2005) 941–950.
[5] L.C. Cruz HG, Applications of two-photon microscopy in the neurosciences, Front. Biosci. 10 (2005) 2263–2278.
[6] M. Rubart, Two-photon microscopy of cells and tissue, Circ. Res. 95 (2004) 1154–1166.
[7] J. Mertz, Nonlinear microscopy: new techniques and applications, Curr. Opin. Neurobiol. 14 (2004) 610–616.
[8] R.P. Haugland, Fluorescence tutorials, Invitrogene Molecular Probes, 2005.
[9] J.R. Lakowicz, Principles of Fluorescence Spectroscopy, Plenum Press, New York, 1999.
[10] N.S. White, R.J. Errington, Fluorescence techniques for drug delivery research: theory and practice, Adv. Drug Del. Rev. 57 (2005) 17–42.

[11] M. Minsky, Memoir on inventing the confocal scanning microscope, Scanning 10 (1988) 128–138.
[12] C. Yang, J. Mertz, Transmission confocal laser scanning microscopy with a virtual pinhole based on nonlinear detection, Opt. Lett. 28 (2003) 224–226.
[13] W. Denk, in: R. Yuste, A. Konnerth (Eds.), Imaging in Neuroscience and Development—A Laboratory Manual, CSHL Press, Cold Spring Harbor, 2005, pp. 53–58.
[14] J. Mertz, in: R. Yuste, A. Konnerth (Eds.), Imaging in Neuroscience and Development—A Laboratory Manual, CSHL Press, Cold Spring Habor, 2005, pp. 71–74.
[15] M. Göppert-Mayer, Über Elementarakete mit zwei Quantensprüngen, Ann. Phys. 9 (1931) 273–294.
[16] W. Kaiser, C. Garret, Two-photon excitation in CaF_2:Eu^{2+}, Phys. Rev. Lett. 7 (1961) 229–231.
[17] W. Denk, J. Strickler, W.W. Webb, Two-photon laser scanning microscope, Science 248 (1990) 73–76.
[18] Z.F. Mainen, M. Maletic-Savatic, S.H. Shi, Y. Hayashi, R. Malinov, K. Svoboda, Two-photon imaging in living brain slices, Methods (Duluth) 18 (1999) 231–239.
[19] M. Müller, J. Schmidt, S.L. Mironov, D.W. Richter, Construction and performance of a custom-built two-photon laser scanning system, J. Phys., D. Appl. Phys. 36 (2003) 1747–1757.
[20] V. Nikolenko, B. Nemet, R. Yuste, A two-photon and second-harmonic microscope, Methods (Duluth) 30 (2003) 3–15.
[21] T.A. Pologruto, B.L. Sabatini, K. Svoboda, ScanImage: flexible software for operating laser scanning microscopes, Biomed. Eng. Online 2 (2003) 13.
[22] E. Beaurepaire, M. Oheim, J. Mertz, Ultra-deep two-photon fluorescence excitation in turbid media, Opt. Commun. 188 (2001) 25–29.
[23] P. Theer, M.T. Hasan, W. Denk, Two-photon imaging to a depth of 1000 μm in living brains by use of a Ti:Al_2O_3 regenerative amplifier, Opt. Lett. 28 (2003) 1022–1024.
[24] A. Hopt, E. Neher, Highly nonlinear photodamage in two-photon fluorescence microscopy, Biophys. J. 80 (2001) 2029–2036.
[25] W. Denk, K. Svoboda, Photon upmanship: why multiphoton imaging is more than a gimmick, Neuron 18 (1997) 351–357.
[26] W. Denk, K.R. Delaney, A. Gelperin, D. Kleinfeld, B.W. Strowbridge, D.W. Tank, R. Yuste, Anatomical and functional imaging of neurons using 2-photon laser scanning microscopy, J. Neurosci. Methods 54 (1994) 151–162.
[27] M. Oheim, E. Beaurepaire, E. Chaigneau, J. Mertz, S. Charpak, Two-photon microscopy in brain tissue: parameters influencing the imaging depth, J. Neurosci. Methods 111 (2001) 29–37.
[28] E. Beaurepaire, J. Mertz, Epifluorescence collection in two-photon microscopy, Appl. Opt. 41 (2002) 5376–5382.
[29] M. Straub, P. Lodemann, P. Holroyd, R. Jahn, S.W. Hell, Live-cell imaging by multifocal multiphoton microscopy, Eur. J. Cell Biol. 79 (2000) 726–734.
[30] R.M. Williams, W. Zipfel, W.W. Webb, Multiphoton microscopy in biological research, Curr. Opin. Chem. Biol. 5 (2001) 603–608.
[31] J.D. Lechtleiter, D.-T. Lin, I. Sieneart, Multi-photon laser scanning microscopy using an acousto-optic deflector, Biophys. J. 83 (2002) 2292–2299.
[32] R. Salome, K.Y., S. Dieudonné, J.F. Leger, O. Krichevsky, C. Wyart, D. Chatenay, L. Bourdieu, Ultrafast random-access scanning in two-photon microscopy using acousto-optic deflectors, J. Neurosci. Methods 154 (1–2) (2006) 161–174.
[33] B.K.A. Ngoi, K. Venkatakrishnan, L.E.M. Lim, T.B., Angular dispersion compensation for acousto-optic devices used for ultrashort-pulsed laser micromachining, Opt. Express 9 (2001) 200–206.
[34] P.M. Delaney, H.M.R., in: J.B. Pawley (Ed.), Handbook of Confocal Microscopy, Plenum, New York, 1995, pp. 515–523.
[35] F. Helmchen, Miniaturization of fluorescence microscopes using fibre optics, Exp. Physiol. 87 (2002) 737–745.
[36] G.P. Agrawal, Nonlinear Fiber Optics, Academic Press, San Diego, 1995.
[37] S.W. Clark, F.Ö. Ilday, F.W. Wise, Fiber delivery of femtosecond pulses from a Ti:sapphire laser, Opt. Lett. 26 (2001) 1320–1322.
[38] W. Göbel, A. Nimmerjahn, F. Helmchen, Distortion-free delivery of nanojoule femtosecond pulses from a Ti:sapphire laser through a hollow-core photonic crystal fiber, Opt. Lett. 29 (2004) 1285–1287.
[39] L. Fu, M. Gu, Double-clad photonic crystal fiber coupler for compact nonlinear optical microscopy imaging, Opt. Lett. 31 (2006) 1471–1473.
[40] F. Helmchen, M.S. Fee, D.W. Tank, W. Denk, A miniature head-mounted two-photon microscope: high-resolution brain imaging in freely moving animals, Neuron 31 (2001) 903–912.
[41] D. Bird, M. Gu, Two-photon fluorescence endoscopy with a micro-optic scanning head, Opt. Lett. 28 (2003) 1552–1554.
[42] J.C. Jung, M. Schnitzer, Multiphoton endoscopy, Opt. Lett. 28 (2003) 902–904.
[43] M.J. Levene, D.A. Dombeck, W.W. Webb, In vivo multiphoton microscopy of deep brain tissue, J. Neurophysiol. 91 (2004) 1908–1912.
[44] L. Fu, X. Gan, M. Gu, Characterization of gradient-index lens-fiber spacing toward applications in two-photon fluorescence, Appl. Opt. 44 (2005) 7270–7274.
[45] I. Bureau, G.M. Shepherd, K. Svoboda, Precise development of functional and anatomical columns in the neocortex, Neuron 42 (2004) 789–801.
[46] G.M. Shepherd, A. Stepanyants, I. Bureau, D. Chklovskii, K. Svoboda, Geometric and functional organization of cortical circuits, Nat. Neurosci. 8 (2005) 782–790.
[47] P.S. Tsai, B. Friedman, A.I. Ifarraguerri, B.D. Thompson, B. Lev-Ram, C.B. Schaffer, Q. Xiong, R.Y. Tsien, J.A. Squier, D. Kleinfeld, All-optical histology using ultrashort laser pulses, Neuron 39 (2003) 27–41.
[48] W. Denk, H. Horstmann, Serial block-face scanning electron microscopy to reconstruct three-dimensional tissue nanostructure, PLoS Biol. 2 (2004) e329.
[49] T. Pons, L. Moreaux, J. Mertz, Photoinduced flip-flop of amphiphilic molecules in lipid bilayer membranes, Phys. Rev. Lett. 89 (2002) 288104.

[50] D.L. Wokosin, C.M. Loughrey, G.L. Smith, Characterization of a range of fura dyes with two-photon excitation, Biophys. J. 86 (2004) 1726–1738.
[51] C. Xu, W. Zipfel, J.B. Shear, R.M. Williams, W.W. Webb, Multiphoton fluorescence excitation. New spectral windows for biological nonlinear microscopy, Proc. Natl. Acad. Sci. U.S.A. 93 (1996) 10763–10768.
[52] K.J. Schafer-Hales, K.D. Belfield, S. Yao, P.K. Frederiksen, J.M. Hales, P.E. Kolattukudy, Fluorene-based fluorescent probes with high two-photon action cross-sections for biological multiphoton imaging applications, J. Biomed. Opt. 10 (2005) 051402.
[53] Z.Q. Liu, Q. Fang, D. Wang, D.X. Cao, G. Xue, W.T. Yu, H. Lei, Trivalent boron as an acceptor in donor-pi-acceptor-type compounds for single- and two-photon excited fluorescence, Chemistry 9 (2003) 5074–5084.
[54] S. Kato, T. Matsumoto, M. Shigeiwa, H. Gorohmaru, S. Maeda, T. Ishi-i, S. Makata, Novel 2,1,3-benzothiadiazole-based red-fluorescent dyes with enhanced two-photon absorption cross-sections, Chemistry 12 (2006) 2303–2317.
[55] L. Porres, O. Mongin, C. Katan, M. Charlot, T. Pons, J. Mertz, M. Blanchard-Desce, Enhanced two-photon absorption with novel octupolar propeller-shaped fluorophores derived from triphenylamine, Org. Lett. 6 (2004) 47–50.
[56] C. Le Droumaguet, O. Mongin, M.H. Werts, M. Blanchard-Desce, Towards "smart" multiphoton fluorophores: strongly solvatochromic probes for two-photon sensing of micropolarity, Chem. Commun. 2005 (2005) 2802–2804.
[57] M. Parent, O. Mongin, K. Kamada, C. Katan, M. Blanchard-Desce, New chromophores from click chemistry for two-photon absorption and tunable photoluminescence, Chem. Commun. (2005) 2029–2031.
[58] N.I. Kiskin, R. Chillingworth, J.A. McCray, D. Piston, D. Ogden, The efficiency of two-photon photolysis of a "caged" fluorophore, *o*-1-(2-nitrophenyl)ethylpyranine, in relation to photodamage of synaptic terminals, Eur. Biophys. J. 30 (2002) 588–604.
[59] O.D. Fedoryak, J.Y. Sul, P.G. Haydon, G.C. Ellis-Davies, Synthesis of a caged glutamate for efficient one- and two-photon photorelease on living cells, Chem. Commun. 29 (2005) 3664–3666.
[60] S. Kantevari, C.J. Hoang, J. Ogrodnik, M. Egger, E. Niggli, G.C. Ellis-Davies, Synthesis and two-photon photolysis of 6-(ortho-nitroveratryl)-caged IP3 in living cells, Chembiochem 7 (2006) 174–180.
[61] R. Hellwarth, P. Christensen, Nonlinear optical microscopic examination of structure in polycrystalline ZnSe, Opt. Commun. 12 (1974) 318–322.
[62] C.J.R. Sheppard, R. Kompfner, J. Gannaway, D. Walsh, Scanning harmonic optical microscope, IEEE J. Quantum Electron. 13E (1977) 100D.
[63] P.J. Campagnola, L.M. Loew, Second-harmonic imaging microscopy for visualizing biomolecular arrays in cells, tissues and organisms, Nat. Biotechnol. 21 (2003) 1356–1360.
[64] C.K. Sun, Higher harmonic generation, Adv. Biochem. Eng. Biotechnol. 95 (2005) 17–56.
[65] L. Moreaux, O. Sandre, S. Charpak, M. Blanchard-Desce, J. Mertz, Coherent scattering in multi-harmonic light microscopy, Biophys. J. 80 (2001) 1568–1574.
[66] N. Moreno, J.A. Feijo, G. Cox, Implementation and evaluation of a detector for forward propagated second harmonic signals, Micron 35 (2004) 721–724.
[67] B.G. Wang, K. König, I. Riemann, R.H. Krieg, K. J., Intraocular multiphoton microscopy with subcellular spatial resolution by infrared femtosecond lasers, Histochem. Cell Biol. 126 (4) (2006) 507–515.
[68] J.G. Lyubovitsky, J.A. Spencer, T.B. Krasieva, B. Andersen, B.J. Tromberg, Imaging corneal pathology in a transgenic mouse model using nonlinear microscopy, J. Biomed. Opt. 11 (2006) 014013.
[69] D.A. Dombeck, K.A. Kasische, H.D. Vishwasrao, M. Ingelsson, B.T. Hyman, W.W. Webb, Uniform polarity microtubule assemblies imaged in native brain tissue by second-harmonic generation microscopy, Proc. Natl. Acad. Sci. U.S.A. 100 (2003) 7081–7086.
[70] T. Boulesteix, E. Beaurepaire, M.P. Sauviat, M.C. Schanne-Klein, Second-harmonic microscopy of unstained living cardiac myocytes: measurements of sarcomere length with 20-nm accuracy, Opt. Lett. 29 (2004) 2031–2033.
[71] P.J. Campagnola, M.-D. Wei, A. Lewis, L.M. Loew, High-resolution nonlinear optical imaging of live cells by second harmonic generation, Biophys. J. 77 (1999) 3341–3349.
[72] L. Moreaux, T. Pons, B. Dambrin, M. Blanchard-Desce, J. Mertz, Electro-optic response of second-harmonic generation membrane potential sensors, Opt. Lett. 28 (2003) 625–627.
[73] T. Pons, L. Moreaux, O. Mongin, M. Blanchard-Desce, J. Mertz, Mechanisms of membrane potential sensing with second-harmonic generation microscopy, J. Biomed. Opt. 8 (2003) 428–431.
[74] A.C. Millard, L. Jin, J.P. Wuskell, D.M. Bourdreau, A. Lewis, L.M. Loew, Wavelength- and time-dependence of potentiometric non-linear optical signals from styryl dyes, J. Membr. Biol. 208 (2005) 103–111.
[75] L. Sacconi, D.A. Dombeck, W.W. Webb, Overcoming photodamage in second-harmonic generation microscopy: real-time optical recording of neuronal action potentials, Proc. Natl. Acad. Sci. U.S.A. 103 (2006) 3124–3129.
[76] M. Nuriya, J. Jiang, B. Nemet, K.B. Eisenthal, R. Yuste, Imaging membrane potential in dendritic spines, Proc. Natl. Acad. Sci. U.S.A. 103 (2006) 786–790.
[77] D. Debarre, W. Supatto, E. Beaurepaire, Structure sensitivity in third-harmonic generation microscopy, Opt. Lett. 30 (2005) 2134–2136.
[78] S.W. Chau, S.P. Tai, C.L. Ho, C.H. Lin, C.K. Sun, High-resolution simultaneous three-photon fluorescence and third-harmonic-generation microscopy, Microsc. Res. Tech. 66 (2005) 193–197.
[79] D. Debarre, W. Supatto, A.M. Pena, A. Fabre, T. Tordjmann, L. Combettes, M.C. Schanne-Klein, E. Beaurepaire, Imaging lipid bodies in cells and tissues using third-harmonic generation microscopy, Nat. Methods 3 (2006) 47–53.
[80] N. Uzunbajakava, C. Otto, Combined Raman and continuous-wave-excited two-photon fluorescence cell imaging, Opt. Lett. 28 (2003) 2073–2075.
[81] N. Billington, A.W. Knight, Seeing the wood through the trees: a review of techniques for distinguishing green

fluorescent protein from endogenous autofluorescence, Anal. Biochem. 291 (2001) 175–197.
[82] M. Duncan, J. Reintjes, T. Manuccia, Scanning coherent anti-Stokes Raman microscope, Opt. Lett. 7 (1982) 350–352.
[83] A. Zumbusch, G.R. Holtom, X.S. Xie, Three-dimensional vibrational imaging by coherent anti-Stokes Raman scattering, Phys. Rev. Lett. 82 (1999) 4142–4145.
[84] J.-X. Cheng, K. Jia, G. Eheng, X.S. Xie, Laser-scanning coherent anti-Stokes Raman scattering microscopy and application to cell biology, Biophys. J. 83 (2002) 502–509.
[85] S.W. Hell, M. Schrader, K. Bahlmann, F. Meinecke, J.R. Lakowicz, I. Gryczynski, Stimulated emission on the microscopic scale: light quenching of pyridine 2 with a Ti:sapphire laser, J. Microsc. 180 (1995) RP1.
[86] M. Schrader, F. Meinecke, K. Bahlmann, M. Kroug, C. Cremer, E. Soini, S.W. Hell, Monitoring the excited state of a fluorophore in a microscope by stimulated emission, Bioimaging 3 (1995) 147–153.
[87] S.W. Hell, M. Dyba, S. Jakobs, Concepts for nanoscale resolution in fluorescence microscopy, Curr. Opin. Neurobiol. 14 (2004) 599–609.
[88] S.W. Hell, Toward fluorescence nanoscopy, Nat. Biotechnol. 21 (2003) 1347–1355.
[89] S.W. Hell, J. Wichmann, Breaking the diffraction resolution limit by stimulated emission: stimulated emission depletion fluorescence microscopy, Opt. Lett. 19 (1994) 780–782.
[90] J.B. Birks, Photophysics of Aromatic Molecules, Wiley Interscience, London, 1970.
[91] V. Westphal, L. Kastrup, S.W. Hell, Lateral resolution of 28 nm (λ/25) in far-field fluorescence microscopy, Appl. Phys., B 77 (2003) 377–380.
[92] T.A. Klar, S. Jakobs, M. Dyba, A. Egner, S.W. Hell, Fluorescence microscopy with diffraction resolution barrier broken by stimulated emission, PNAS 97 (2000) 8206–8210.
[93] V. Westphal, S.W. Hell, Nanoscale resolution in the focal plane of an optical microscope, Phys. Rev. Lett. 94 (2005) 14903.
[94] A.J. Bain, R.J. Marsh, D.A. Armoogum, O. Mongin, L. Porres, M. Blanchard-Desce, Time-resolved stimulated emission depletion in two-photon excited states, Biochem. Soc. Trans. 31 (2003) 1047–1051.
[95] K.I. Willig, S.O. Rizzoli, V. Westphal, R. Jahn, S.W. Hell, STED microscopy reveals that synaptotagmin remains clustered after synaptic vesicle exocytosis, Nature 440 (2006) 935–939.
[96] J.J. Sieber, K.I. Willig, R. Heintzmann, S.W. Hell, T. Lang, The SNARE motif is essential for the formation of syntaxin clusters in the plasma membrane, Biophys. J. 90 (2006) 2843–2851.
[97] R.J. Kittel, C. Wichmann, T.M. Rasse, W. Fouquet, M. Schmidt, A. Schmdt, D.A. Wagh, C. Pawlu, R.R. Kellner, K.I. Willig, S.W. Hell, E. Buchner, M. Heckmann, S.J. Sigrist, Bruchpilot promotes active zone assembly, Ca^{2+} channel clustering, and vesicle release, Science 312 (2006).
[98] I. Gryczynski, Z. Gryczynski, L.J. R., Two-photon excitation by the evanescent wave from total internal reflection, Anal. Biochem. 247 (1997) 69–76.
[99] G.L. Duveneck, M.A. Bopp, M. Ehrat, M. Haiml, U. Keller, M.A. Bader, G. Marowsky, S. Soria, Evanescent-field-induced two-photon fluorescence: excitation of macroscopic areas of planar waveguides, Appl. Phys., B 73 (2001) 869–871.
[100] F. Schapper, J.T. Goncalves, M. Oheim, Fluorescence imaging with two-photon evanescent wave excitation, Eur. Biophys. J. 32 (2003) 635–643.
[101] S. Soria, K.N. Thayil, G. Badenes, M.A. Bader, A. Selle, G. Marowsky, Resonant double grating waveguide structures as enhancement platforms for two-photon fluorescence excitation, Appl. Phys. Lett. 87 (2005) 1–3.
[102] A. Selle, C. Kappel, M.A. Bader, G. Marowsky, K. Winkler, U. Alexiev, Picosecond-pulse-induced two-photon fluorescence enhancement in biological material by application of grating waveguide structures, Opt. Lett. 30 (2005) 1683–1685.
[103] T. Fricke-Begemann, B.M. A., J. Ihlemann, C. Kappel, G. Marowsky, J. Meinertz, S.A., Two-photon fluorescence: large-area excitation and enhanced sensitivity using waveguide structures, 106. Conference, Deutsche Gesellschaft fuer angewandte Optik, 2005.
[104] V.G. Bordo, J. Loerke, H.G. Rubahn, Two-photon evanescent-volume wave spectroscopy: a new account of gas–solid dynamics in the boundary layer, Phys. Rev. Lett. 86 (2001) 1490–1493.
[105] Z. Huang, N.L. Thompson, Theory for two-photon excitation in pattern photobleaching with evanescent illumination, Biophys. Chem. 47 (1993) 241–249.
[106] J.W. Chon, M. Gu, C. Bullen, P. Mulvaney, Two-photon fluorescence scanning near-field microscopy based on a focused evanescent field under total internal reflection, Opt. Lett. 28 (2003) 1930–1932.
[107] J.W. Chon, M. Gu, Scanning total internal reflection fluorescence microscopy under one-photon and two-photon excitation: image formation, Appl. Opt. 43 (2004) 1063–1071.
[108] M. Oheim, F. Schapper, Non-linear evanescent-field imaging, J. Phys., D Appl. Phys. 38 (2005) R185–R197.
[109] D. Axelrod, Methods in Enzymology, Academic Press, San Diego, 2003.
[110] A.L. Stout, D. Axelrod, Evanescent field excitation of fluorescence by epi-illumination microscopy, Appl. Opt. 28 (1989) 5237–5242.
[111] A. Mattheyses, D. Axelrod, Direct measurement of the evanescent field profile produced by objective-based total internal reflection fluorescence, J. Biomed. Opt. 11 (2006) 014006.
[112] R. Lansford, G. Bearman, S.E. Fraser, Resolution of multiple green fluorescent protein color variants and dyes using two-photon microscopy and imaging spectroscopy, J. Biomed. Opt. 6 (2001) 311–318.
[113] M. Kiguchi, et al., New method of measuring second harmonic generation efficiency using powder crystals, Appl. Phys. Lett. 60 (16) (1992) 1933–1935.
[114] N. Bloembergen, P.S. Pershan, Light waves at the boundary of nonlinear media, Phys. Rev. 128 (2) (1962) 602–622.